ACSNANO
www.acsnano.org
ARTICLE

Exploring High-Performance n-Type Thermoelectric Composites Using Amino-Substituted Rylene Dimides and Carbon Nanotubes

Guangbao Wu,[†,‡] Zhi-Guo Zhang,[†] Yongfang Li,[†] Caiyan Gao,[*,†] Xin Wang,[*,‡] and Guangming Chen[*,†]

[†]Institute of Chemistry, Chinese Academy of Sciences, Beijing 100190, P. R. China

[‡]Key Laboratory of Rubber-Plastics, Ministry of Education, Qingdao University of Science and Technology, Qingdao 266042, P. R. China

Supporting Information

ABSTRACT: Taking advantage of the high electrical conductivity of a single-walled carbon nanotube (SWCNT) and the large Seebeck coefficient of rylene diimide, a convenient strategy is proposed to achieve high-performance n-type thermoelectric (TE) composites containing a SWCNT and amino-substituted perylene diimide (PDINE) or naphthalene diimide (NDINE). The obtained n-type composites display greatly enhanced TE performance with maximum power factors of 112 ± 8 (PDINE/SWCNT) and 135 ± 14 (NDINE/SWCNT) μW m^{-1} K^{-2}. A short doping time of 0.5 h can ensure high TE performance. The corresponding TE module consisting of five p−n junctions reaches a large output power of 3.3 μW under a 50 °C temperature gradient. In addition, the n-type composites exhibit high air stability and excellent thermal stability. This design strategy benefits the future fabricating of high-performance n-type TE materials and devices.

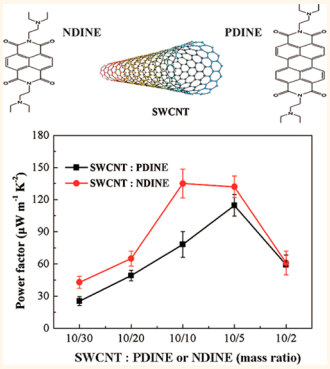

KEYWORDS: *thermoelectric, n-type, composite, single-walled carbon nanotube, amino-substituted rylene diimide*

Enhancement in the efficiency of energy use is urgent, particularly with the background of fossil energy exhaustion, since the heat generated in industrial production and daily lives is mostly dissipated and wasted.[1] Thermoelectric (TE) materials can realize direct energy conversion between electricity and heat, being very attractive in harvesting low-quality or waste heat.[2] Recently, organic and the organic/inorganic composite TE materials have received great attention due to their mechanical flexibility, low thermal conductivity, and no moving parts or bulk fluids.[3−11] Considering their low thermal conductivities, high power factor (PF, defined as $S^2\sigma$, where S and σ represent the Seebeck coefficient or thermopower and the electrical conductivity, respectively) is strongly desired for organic and organic/inorganic composite materials, and thus PF is often employed to evaluate the TE performance.[3−11] In the past several years, great progresses have been made for p-type TE composites, especially conducting polymer/carbon particle composites, including poly(3,4-ethylenedioxythiophene) (PEDOT), polyaniline (PANI), and polypyrrole (PPy) with carbon nanotubes (CNTs) or graphene.[12−17] Several donor−acceptor systems have also been developed for their TE applications.[18,19] In sharp contrast, n-type organic/inorganic TE composites still remain a great challenge.

To date, few n-type organic/inorganic composite TE materials concentrate on the preparation by doping of pristine CNTs or grapheme (p-type) by a reducing agent with electron donors, such as poly(ether imide) (PEI)),[20,21] or small organic molecules (for instance triphenylphosphine (tpp)).[21,22] For example, Nonoguchi and Kawai *et al.*[21] systematically studied the conversion of single-walled CNTs (SWCNTs) with n-type characteristics using a series of small organic molecules or polymers.[21] Recently, we have reported high-performance organic TE modules based on flexible films of n-type SWCNTs obtained by diethylenetriamine (DETA) doping with subsequent calcium hydride (CaH_2) treatment.[22] However, carbon-based materials doped by insulated organic dopants are usually unstable in air and show low or medium power factors.

Small molecules or organic polymers with large Seebeck coefficients are an attractive candidate in n-type organic TE

Received: February 23, 2017
Accepted: May 16, 2017
Published: May 16, 2017

DOI: 10.1021/acsnano.7b01279
ACS Nano 2017, 11, 5746−5752

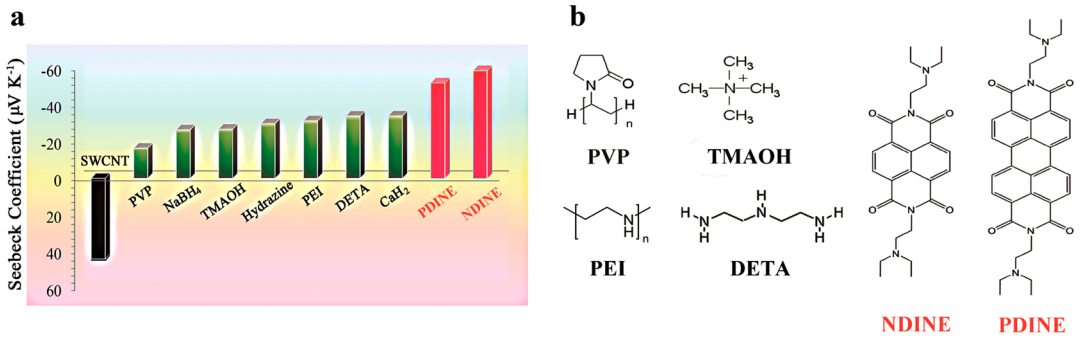

Figure 1. (a) Seebeck coefficients of the films of the pristine SWCNT and the SWCNTs reduced by various inorganic, organic, or polymer chemicals. (b) Molecular structures of some organic reducing molecules or polymers.

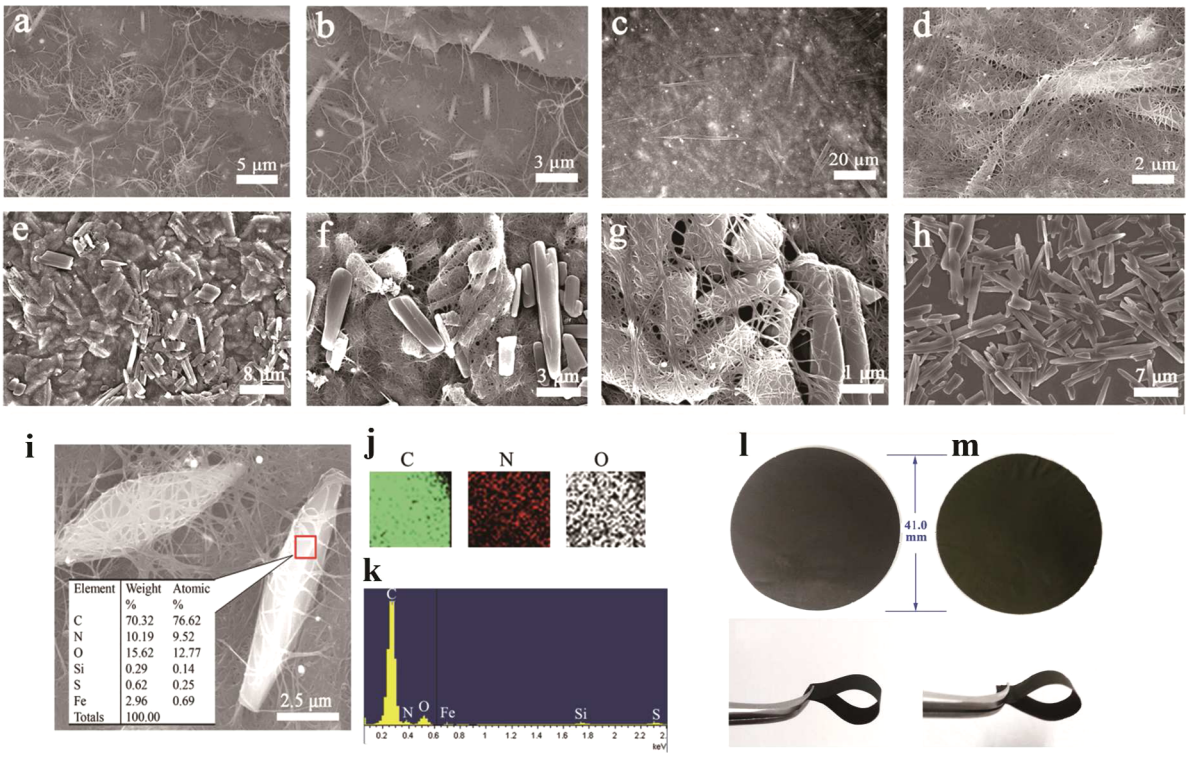

Figure 2. (a–h) FESEM images of the film surfaces: (a–d) the NDINE/SWCNT composites with SWCNT:NDINE mass ratios of (a and b) 10:2 and (c and d) 10:20; (e–g) the PDINE/SWCNT composites with a SWCNT:PDINE mass ratio of 10:10; (h) pure PDINE. (i) Crystal's EDS area scan for PDINE/SWCNT composite with an inset of element weight or atomic percentages. (j) Elemental mapping distributions of carbon C, nitrogen N, and oxygen O. (k) Point scanning by EDS. Photographs of (l) NDINE/SWCNT and (m) PDINE/SWCNT composite films displaying high flexibility.

materials.[23−25] Nevertheless, their low electrical conductivities seriously limit the realization of high power factors. Recently, rylene dimides have become a hot topic in wide application fields of photovoltaic cells, organic p−n junctions, n-channel field-effect transistors, *etc.*, mainly due to their high electron affinities and excellent thermal and oxidative stabilities.[26,27] In addition, they are air stable, easily solution processed, environmentally friendly, and highly tunable in functioning efficiency. Chabinyc, Hawker, Segalman, and co-workers reported a preliminary study of TE applications of perylene diimide (PDI) derivatives with varying alkyl lengths.[28] Although the compounds display large Seebeck coefficients, their low electrical conductivities ($\leq$0.5 S cm^{-1}) lead to a low power factor maximum of only 1.4 μW m^{-1} K^{-2}. Theoretically, it is viable to achieve a high electrical conductivity and power factor by judicious incorporation of a 3D interconnected network of inorganic nanoparticles with high electrical conductivities. To conduct this strategy, we design amino-substituted rylene derivatives of PDI (PDINE) and naphthalene diimide (NDINE) and then construct the architecture of well-dispersed PDINE or NDINE crystals in SWCNT networks. The composites of PDINE/SWCNT and NDINE/SWCNT display greatly enhanced TE performance with the maximum power factors of 112 $\pm$ 8 and 135 $\pm$ 14 μW m^{-1} K^{-2}, respectively, which are among the highest for organic/inorganic TE composites reported so far. Moreover, the corresponding TE module consisting of five p−n junctions generates a large output power of 3.3 μW under a 50 °C temperature gradient. In addition, the n-type composites exhibit high air stability and excellent thermal stability.

DOI: 10.1021/acsnano.7b01279
ACS Nano 2017, 11, 5746−5752

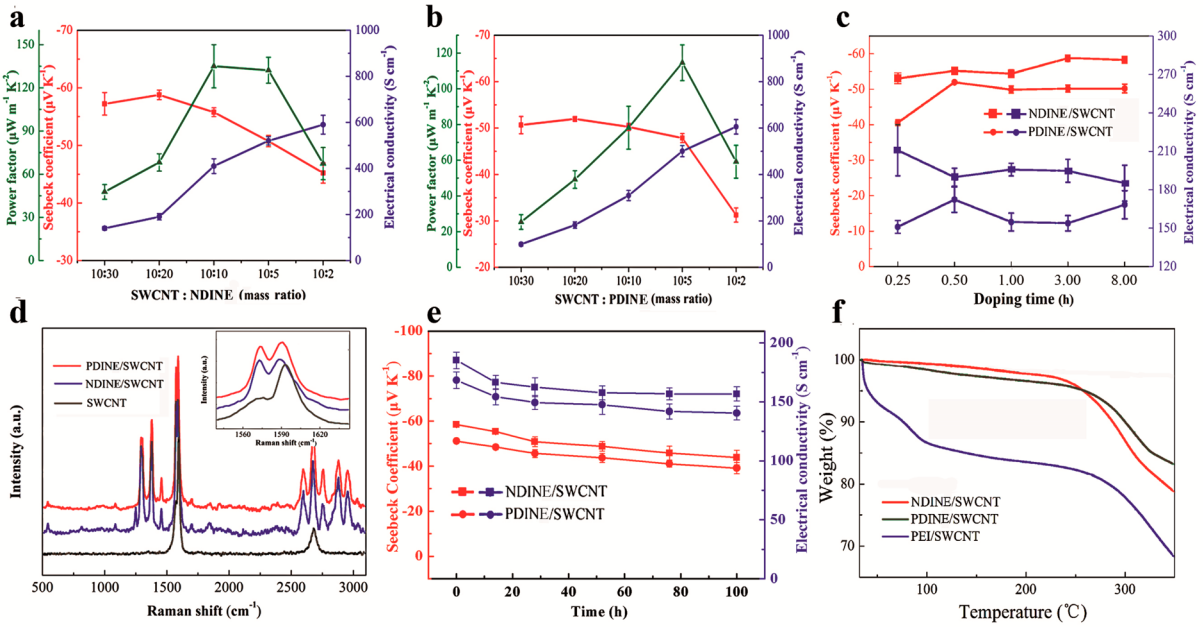

Figure 3. Seebeck coefficients, electrical conductivities, and power factors at room temperature for (a) NDINE/SWCNT and (b) PDINE/SWCNT composite films with different mass ratios (the doping time was 3 h). (c) Dependence of Seebeck coefficients and electrical conductivities for the composites with doping time (the mass ratio of NDINE/SWCNT or PDINE/SWCNT was 20:10). (d) Raman spectra of PDINE/SWCNT composite, NDINE/SWCNT composite and pure SWCNT. (e) The air stability of the composites exposed at room temperature. (f) TGA curves of NDINE/SWCNT, PDINE/SWCNT, and PEI/SWCNT composites in nitrogen atmosphere.

RESULTS AND DISCUSSION

The synthesized PDINE and NDINE are characterized by ^{1}H NMR and FTIR spectra (shown in Figures S1−3, Supporting Information). The composites of PDINE/SWCNT and NDIDE/SWCNT were obtained by a convenient solution mixing method. Figure 1a compares the SWCNT p- to n-type transition using PDINE, NDINE, and some widely reported reducing agents including inorganic (sodium borohydride ($NaBH_4$), hydrazine, and CaH_2), organic (tetramethylammonium hydroxide (TMAOH), DETA), and polymer (polyvinylpyrrolidone (PVP) and PEI) materials. Figure 1b illustrates the chemical structures of PVP, TMAOH, PEI, DETA, NDIDE, and PDINE. Due to oxygen doping in air and/or defects during the preparation process, the pristine CNTs usually exhibit p-type semiconducting characteristics.[29−31] The SWCNT used in the present study displays a positive Seebeck coefficient of 43.0 ± 2.0 μV K^{-1}. Distinctly, all of the reduced SWCNTs by inorganic, organic, or polymer chemicals exhibit negative Seebeck coefficients, demonstrating the success of the p- to n-type transition. Furthermore, the Seebeck coefficients for the composites of PDINE/SWCNT and NDINE/SWCNT reveal large thermopowers of −52.4 ± 0.2 and −60.2 ± 0.4 μV K^{-1}, respectively, much larger than the SWCNTs doped by any other typical reducing agents. More importantly, these composites have high electrical conductivities, *i.e.*, 500 ± 15 S cm^{-1} for the PDINE/SWCNT (mass ratio 5:10) and 400 ± 17 S cm^{-1} for the NDIDE/SWCNT (mass ratio 10:10). Consequently, the PDINE/SWCNT and NDIDE/SWCNT composites display high power factors of 112 ± 8 and 135 ± 14 μW m^{-1} K^{-2}, respectively, 80 and ∼96 times of that of the previous reported 1.4 μW m^{-1} K^{-2} for PDI.[28] Therefore, we conclude that the PDINE/SWCNT and NDINE/SWCNT composites reported herein are excellent n-type TE composites, which can be employed to further fabricate high-performance TE devices.

Figure 2a−h shows the morphological observations of the NDINE/SWCNT and PDINE/SWCNT composites by field-emission scanning electron microscopic (FESEM) images. The well-dispersed rod-like crystals are the aggregates of the organic molecules (NINDE or PDINE), wrapped by a 3D interconnected SWCNT network due to strong $\pi-\pi$ interfacial interactions. The crystalline behavior for NDINE and PDINE can also be confirmed by a series of sharp diffraction peaks in the X-ray diffraction (XRD) patterns (Figure S4). Moreover, the rod-like crystals grow larger with the reduction of SWCNT:NDINE mass ratios (Figure 2a−d), possibly due to the increased NDINE content. The NDINE crystals in the NDINE/SWCNT composite at a SWCNT:NDINE mass ratio of 10:2 reveal an average length and width of 3.0 and 0.6 μm, respectively. At a high mass ratio of 10:10, the average length and width increase to 25.0 and 1.0 μm, respectively. A similar morphology is also observed for the PDINE/SWCNT composite (Figure 2e−g), while individual PDINE crystals are prevalent in Figure 2h. The main morphology deviance lies in the larger crystals with an average width of 2.0 μm which are more prevalent in the PDINE/SWCNT (Figure 2e−h) than in the NDINE/SWNCT composites (Figure 2a−d), possibly due to the high crystallization capability of PDINE than that of NDINE. Figure 2h shows the large crystals of pure PDINE; in contrast, no NDINE crystals can be clearly recognized, as obtained under the same preparation conditions.

In order to ensure that the rod-like crystals are resulted from PDINE or NDINE rather than inorganic salts, we carried out the microscopic elemental analysis by energy dispersive spectrometer (EDS), taking PDINE/SWCNT as an example (Figure 2i−k). Distinctly, the element weight or atomic percentage (the inset of i), the elemental mappings of C, N, and O (Figure 2j), and the point scanning (Figure 2k) provide

DOI: 10.1021/acsnano.7b01279
ACS Nano 2017, 11, 5746−5752

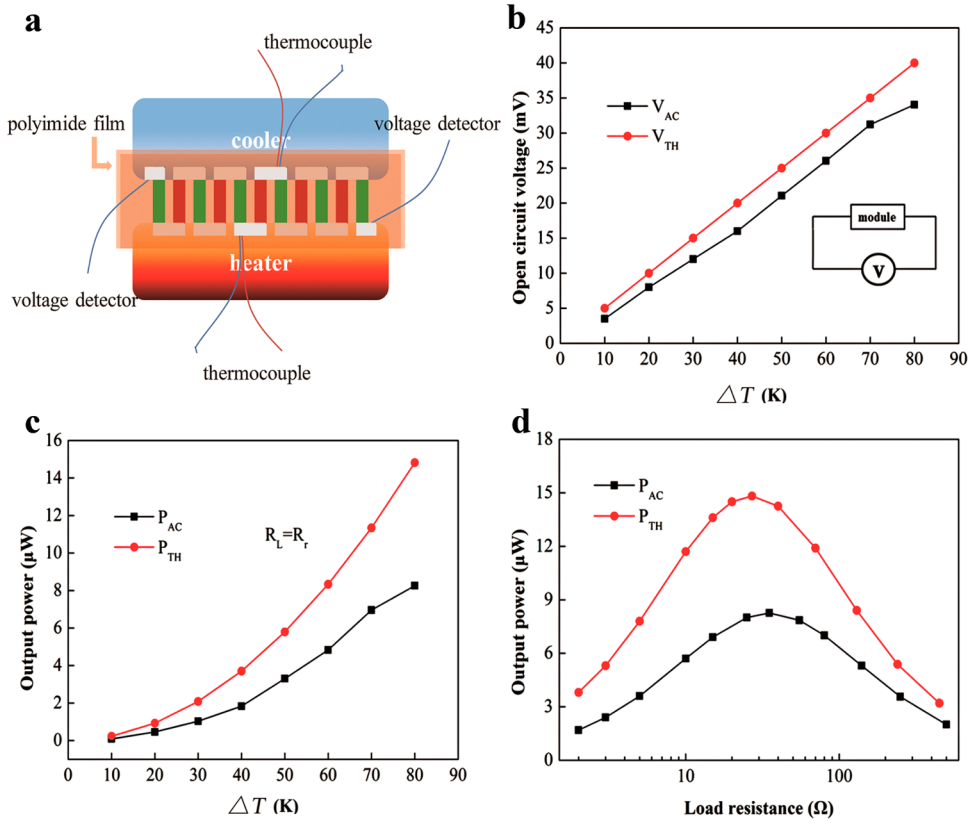

Figure 4. (a) Schematic illustration of a TE module consisting of five p−n junctions for detecting. (b) Open circuit voltage and (c) output power generated from the module consisting of five p−n junctions as a function of temperature gradient (ΔT). (d) Output power generated from the module consisting of five p−n junctions as a function of load resistance at ΔT = 80 °C.

solid proof. Indeed, the proportions of C, N, and O components (Figure 2i) agree very well with the corresponding theoretically calculated values of PDINE, while small amounts of Fe and S elements result from the catalyst residues in SWCNT preparation and the remaining solvent of dimethyl sulfoxide (DMSO) during the composite preparation. Additionally, the elemental analyses (Table S1), the FTIR spectra (Figure S3), and the XRD patterns (Figure S4) further demonstrate that the obtained products contain PDINE or NDINE crystals, rather than inorganic crystals.

Figure 2l,m reveals the PDINE/SWCNT and NDINE/SWCNT composite films with a diameter of ∼41.0 mm and a uniform thickness. The slight color deviance between the two composite films may result from the color difference between NDINE and PDINE. Both the diameter and the thickness can be conveniently adjusted by tuning the filter paper size and the composite amount during the filtration process. Importantly, the NDINE/SWCNT or PDINE/SWCNT composite films display high mechanical flexibility, which can endure a high degree of bending without any obvious breakage or damage. The high flexibility enables the possibility of their applications in wearable electronics or complex conditions.

Figure 3 shows the TE performance and its stabilities for the NDINE/SWCNT and PDINE/SWCNT composites. In Figure 3a,b, both composites share similar trends for the TE performance as a function of SWCNT content. With the increase of the SWCNT:NDINE or SWCNT:PDINE mass ratio, the electrical conductivities increase monotonically, while the Seebeck coefficients first increase slightly and then decrease. As a consequence, the power factors first enhance abruptly and subsequently decrease with increasing mass ratios. Due to the low intrinsic electrical conductivities, the Seebeck coefficients for the pure NDINE and PDINE molecules are difficult to measure. Fortunately, the addition of high electrically conductive SWCNT results in remarkably improved electrical conductivities with a maximum of ∼600 S cm^{-1}. The highest power factors for the PDINE/SWCNT and NDINE/SWCNT composites can reach 112 ± 8 And 135 ± 14 $\mu W\ m^{-1}\ K^{-2}$, respectively, much higher than the n-type SWCNTs doped by a variety of inorganic, organic, and polymer dopants (with a maximum of ∼25 $\mu W\ m^{-1}\ K^{-2}$).[21] To our knowledge, these are among the highest TE performances for n-type organic and organic/inorganic hybrid TE materials.

A short doping period is important and has an obvious advantage for large-scale production. Nevertheless, a long doping time is always required for conventional fabrication of n-type TE composites. For example, a long PEI doping time of 48 h is needed to acquire n-type SWCNT.[32] Excitingly, in the present study, a short doping period of only 0.5 h is enough to realize a significant p- to n-type transition (Figure 3c). Moreover, both the Seebeck coefficients and the electrical conductivities for the doped NDINE/SWCNT and PDINE/SWCNT composites are almost constant, independent of the doping time. Additionally, in the Raman spectra of the pristine SWCNT and the n-type composite SWCNTs (NDINE/SWCNT and PDINE/SWCNT) shown in Figure 3d, the G-band of SWCNT is obviously blue-shifted from 1595 to 1588 cm^{-1}, which has often been observed for the n-type doped SWCNTs.[33]

DOI: 10.1021/acsnano.7b01279
ACS Nano 2017, 11, 5746−5752

When being either exposed in air or heated, the n-type characteristics of organic or composite materials are generally unstable, which is a major hurdle in the applications. For example, PEI-doped SWCNT began to lose weight at a low temperature of even 40 °C.[34] Excitingly, the two composite films reported herein reveal high stability in air (Figure 3e) and excellent thermal stability (Figure 3f). In Figure 3e, after being exposed in air for as long as 100 h, approximately 84.7% and 83.5% of the electrical conductivities could still remain for the NDINE/SWCNT and the PDINE/SWCNT composite films, respectively. As for the Seebeck coefficients, around 75.1% and 70.0% were kept for the NDINE/SWCNT and the PDINE/SWCNT composites as well. On the other hand, Figure 3f demonstrates that the NDINE/SWCNT and PDINE/SWCNT composites exhibit significantly enhanced thermal stabilities relative to that of conventional n-type PEI/SWCNT composite. The PEI/SWCNT composite displays a distinct degradation (~13.4 wt % loss) at low temperatures below 100 °C. In sharp contrast, both n-type composites in the present study had little mass loss at temperatures under 100 °C. At high temperatures, both composites display remarkably improved thermal stabilities than the PEI/SWNCT composite. At 200 °C, *ca.* 97.8 and 96.6 wt % were kept for the NDINE/SWCNT and PDINE/SWCNT composites, respectively. In contrast, only ~83.5 wt % remained for the PEI/SWCNT composite. The onset degradation temperatures (T_{onset}) for the PDINE/SWCNT and NDINE/SWCNT composites are 230 and 245 °C, respectively. Indeed, the residue masses of both composites are higher than those of their corresponding neat organic matrices at high temperatures (shown in Figure S5). Therefore, we conclude that the PDINE/SWCNT and NDINE/SWCNT composites reveal a high stability in air and an excellent thermal stability upon heating. Their stable TE performances will greatly facilitate their applications. More importantly, the high thermal stability at high temperatures means that a large temperature gradient can be applied to the TE device to obtain large output voltage and power, which are very beneficial to device applications.

In order to generate a sufficient power output, p- and n-type TE materials are combined to fabricate TE modules.[8] Figure 4a displays a schematic illustration of a TE module consisting of five p−n junctions, and a photograph of the real module is presented in Figure S6. Here, the SDBS-doped SWCNT (σ, S, and power factor are around 650 S cm^{-1}, 43 μV K^{-1}, and 120 μW m^{-1} K^{-2}, respectively) was used as the p-type TE component, while the NDINE/SWCNT composite film with a power factor of 135 ± 14 μW m^{-1} K^{-2} was employed as the n-type one. All of the p- and n-type films were cut into rectangular strips and interconnected by aluminum foil and silver paste. Thermocouple (Cu) wires were embedded to detect the temperature difference (ΔT) between the hot and cool ends of the module. Ohmic contacts were established, confirmed by the linear characteristic of the I−V curves shown in Figures S7 and S8. First, open circuit voltages of the TE modules were measured as a function of temperature gradients (Figure 4b). The actual voltages (V_{AC}) were measured, and the theoretical voltages (V_{TH}) despite the voltage drop at connection were compared and calculated according to eq 1:

$$V_{TH} = n(S_n + S_p) \times \Delta T \quad (1)$$

where n, S_n, S_p are the number of the p−n junctions and the Seebeck coefficients of n- and p-type components, respectively. As shown in Figure 4b, the V_{AC} increases essentially linearly with ΔT and is almost comparable to the V_{TH}. At ΔT = 50 °C, a V_{AC} of 22 mV was measured, much higher than those reported previously.[32,35]

Given the Seebeck coefficients, the actual TE output powers (P_{AC}) can be obtained and compared with the theoretically expected values (P_{TH}). In particular, when the internal resistance (R_r) equals the load resistance (R_L), the output power *versus* R_L reaches its maximum for a given number of p−n junctions, as shown by the peaks in Figure 4d. As R_L increases above R_r, the output power decreases gradually toward zero as R_L= ∝. This behavior is the result of the dependence of output power on R_L, as described by the following eqs 2 and 3:

$$P_{AC} = \frac{V_{AC}^2 R_L}{(R_r + R_L)^2} = \frac{V_{AC}^2}{\frac{(R_r - R_L)^2}{R_L} + 4R_r} \quad (2)$$

$$P_{TH} = \frac{V_{TH}^2 R_L}{(nr_n + nr_p + R_L)^2} = \frac{V_{TH}^2}{\frac{(nr_n + nr_p - R_L)^2}{R_L} + 4n(r_n + r_p)} \quad (3)$$

where r_n and r_p are the resistances of n- and p-type films, respectively. The internal resistance (R_r = 37.0 Ω, including connector resistance) and the resistances of n-type (r_n = 3.2 Ω) and p-type films (r_p = 1.3 Ω) were measured by a standard four probe method. Thus, P_{AC} and P_{TH} can be obtained as a function of temperature gradient and load resistance, as shown in Figure 4c,d. For example, when the TE module consisting of five p−n junctions was under a 50 °C temperature gradient, a maximum value of P_{AC} = 3.3 μW was calculated, higher than those of the previous reports.[20,36] As expected, the P_{AC} of the TE module at room temperature is among the highest values for TE devices reported so far.

CONCLUSION

We report an example of high-performance n-type TE composites by the combination of highly electrically conductive SWCNTs with PDINE or NDINE. A morphology of well-dispersed PDINE or NDINE crystals in 3D interconnected SWCNT networks is observed. A short doping time of 0.5 h can ensure the high TE performance, which is an advantage over most previous research. The TE composites of PDINE/SWCNT and NDINE/SWCNT exhibit a maximum power factor of 112 ± 8 and 135 ± 14 μW m^{-1} K^{-2}, respectively. The corresponding TE module consisting of five couples of p- and n-type components displays the optimum output power of 3.3 μW under 50 °C temperature gradient. The power factor for the composite and the output power for the TE module are among the highest values for n-type organic/inorganic TE composites reported so far. Furthermore, the PDINE/SWCNT and the NDINE/SWCNT composite films reveal a high stability in air and an excellent thermal stability upon heating. This design strategy benefits the fabrication of high-performance n-type TE materials and devices and is promising in speeding up the TE applications of organic/inorganic composites.

METHODS

Materials. A commercialized SWCNT with a purity >85.0 wt % was bought from Shenzhen Nanotech Port Co. Ltd., China and prepared by chemical vapor deposition (CVD). 3,4,9,10-Perylenetetracarboxylic dianhydride and 1,4,5,8-naphthalenetetracarboxylic dianhydride were purchased from Aldrich, while *N*,*N*-diethylethylenedi-

DOI: 10.1021/acsnano.7b01279
ACS Nano 2017, 11, 5746−5752

amine and imidazole were bought from J&K. Other main chemical reagents, including tetramethylammonium hydroxide (TMAOH), poly(ether imide) (PEI), triphenylphosphine (tpp), and diethylenetriamine (DETA) were purchased from Aldrich.

PDINE and NDINE Syntheses. 3,4,9,10-Perylenetetracarboxylic dianhydride (1.082 g, 2.757 mmol) or 1,4,5,8-naphthalenetetracarboxylic dianhydride (0.74 g, 2.757 mmol) and the *N*,*N*-diethylethylenediamine (0.986 g, 11.2 mmol) were mixed with imidazole (14.1 g, 207 mmol) in a round-bottom flask equipped and sealed with a septum. The reaction vessel was purged with nitrogen and subsequently heated while magnetically stirring at 130 °C for 2 h. Then, the vessel was allowed to cool to room temperature, and the contents were suspended in methanol. Finally, the solid was collected by filtration using a nylon membrane (pore diameter: 0.45 μm), washed with methanol, and dried under vacuum. ^{1}H NMR (400 MHz, $CDCl_3$, δ, ppm) for PDINE: 1.16 (t, J = 1.4 Hz, 12H), 2.77−2.78 (m, 8H), 2.91 (t, J = 1.6 Hz, 4H), 4.37 (t, J = 1.2 Hz, 4H), 8.59 (d, J = 1.2 Hz, 4H), 8.65 (d, J = 0.8 Hz, 4H). ^{1}H NMR (400 MHz, $CDCl_3$, δ, ppm) for NDINE: 1.05 (t, J = 9.4 Hz, 12H), 2.61−2.66 (m, 8H), 2.79 (t, J = 9.8 Hz, 4H), 4.31 (t, J = 9.6 Hz, 4H), 8.75 (s, J = 1.2 Hz, 4H).

Composite Film Preparation. A typical preparation procedure of the n-type composite film (PDINE/SWCNT or NDINE/SWCNT) is described in the following. First, 10 mg of SWCNT was added into 20 mL of DMSO solution containing a desired amount of PDINE or NDINE and ultrasonically treated different times (0.25, 0.5, 1, 3, 8h) for doping periods. After that, the mixture was vacuum filtered by nylon membrane (pore diameter: 0.45 μm) to achieve composite film with 10 μm thickness. Finally, the obtained film was dried under vacuum at 50 °C for 4 h. As for the p-type composite film, 30 mg of SDBS and 10 mg of SWCNT were dispersed in 30 mL of ethanol under ultrasonic treatment for 60 min. The mixture was vacuum filtered and subsequently dried under vacuum at 80 °C for 40 min to obtain a p-type film.

Fabrication of TE Modules. The films used for TE measurements for p- and n-type materials were in a rectangular shape with dimensions of 20 mm × 6 mm and interconnected by aluminum foil and silver paste. Thermocouple (Cu) wires were embedded between the hot and cool ends of the module for detecting real-time temperature. Two wires (Cu) were connected to the ends of TE module for measuring the output voltage.

Measurements. The electrical conductivities and the Seebeck coefficients at room temperature were measured by a commercial instrument, Film Thermoelectric Parameter Test System (Namicro-F3), JiaYiTong Company. During the measurements, a quasi-steady-state mode was adopted. The resistances were measured by Keithley 192 Programmable DMM. The output voltage and power of TE module were measured using a Keithley 2000 Multimeter (Keithley Instruments Inc., USA). Raman spectra were recorded within the wavenumber range of 500−3100 cm^{-1} through a Raman spectrometer (Renishaw inVia plus) with an excitation wavelength of 514 nm. The element mappings and morphologies of the composite films were observed using a field-emission scanning electron microscope (HITACHI S-4800). Thermogravimetric analyses (TGA) of the composites were measured under nitrogen atmosphere by Synchronous Thermal Analyzer Q600 at a heating rate of 10 °C min^{-1}. Fourier transform infrared (FTIR) spectra were collected with a PerkinElmer System 2000 FTIR spectrophotometer with 32 scans in the wavenumber range of 4000−400 cm^{-1}. The morphology was directly observed using a HITACHI S-4800 scanning electron microscope at an acceleration voltage of 15 kV. Powder XRD measurements were carried out using a Rigaku D/max 2400 diffractometer with Cu Kα radiation (λ = 0.15418 nm) at a scanning rate of 10° min^{-1}.

ASSOCIATED CONTENT

Supporting Information

The Supporting Information is available free of charge on the ACS Publications website at DOI: 10.1021/acsnano.7b01279.

Figures S1 and S2: ^{1}H NMR spectrum of PDINE and NDINE (400 MHz, CDCl3); Figure S3: FTIR spectra of NDINE, PDINE, SWCNT, and composites of NDINE/SWCNT or PDINE/SWCNT; Figure S4: XRD patterns of NDINE, PDINE, NDINE/SWCNT composite and PDINE/SWCNT composite; Figure S5: TGA curves of the neat SWCNT, the neat NDINE, and the neat PDINE; Figure S6: A photograph of the TE module made up of five couples of p- and n-type films; Figures S7 and S8: The I−V curve of the n-type film of the NDINE/SWCNT or PDINE/SWCNT composite with Al foil as electrical conductive wires; Table S1: Elemental analyses of SWCNT, NDINE/SWCNT, and PDINE/SWCNT composites (PDF)

AUTHOR INFORMATION

Corresponding Authors

*E-mail: chengm@iccas.ac.cn.
*E-mail: gaocaiyan@iccas.ac.cn.
*E-mail: wangxin@qust.edu.cn.

ORCID

Zhi-Guo Zhang: 0000-0003-4341-7773
Yongfang Li: 0000-0002-2565-2748
Guangming Chen: 0000-0002-9848-9101

Notes

The authors declare no competing financial interest.

ACKNOWLEDGMENTS

We thank the financial support of the National Natural Science Foundation of China (51573190), State Key Development Program for Basic Research of China (2011CB932801), and Key Research Development of Shandong province, China (2015GGX102002). G.C. and Z.Z. thank the Youth Innovation Promotion Association, Chinese Academy of Sciences (2012024 and 2017044).

REFERENCES

(1) Chen, X.; Li, C.; Grätzel, M.; Kostecki, R.; Mao, S. Nanomaterials for Renewable Energy Production and Storage. *Chem. Soc. Rev.* **2012**, *41*, 7909−7937.

(2) Chere, E. K.; Zhang, Q.; McEnaney, K.; Yao, M.; Cao, F.; Sun, J.; Chen, S.; Opeil, C.; Chen, G.; Ren, Z. Enhancement of Thermoelectric Performance in N-type $PbTe_{1-y}Se_y$ by Doping Cr and Tuning Te:Se Ratio. *Nano Energy* **2015**, *13*, 355−367.

(3) Meng, C.; Liu, C.; Fan, S. A Promising Approach to Enhanced Thermoelectric Properties Using Carbon Nanotube Networks. *Adv. Mater.* **2010**, *22*, 535−539.

(4) Bubnova, O.; Khan, Z. U.; Wang, H.; Braun, S.; Evans, D. R.; Fabretto, M.; Hojati-Talemi, P.; Dagnelund, D.; Arlin, J.-B.; Geerts, Y. H.; Desbief, S.; Breiby, D. W.; Andreasen, J. W.; Lazzaroni, R.; Chen, W. M.; Zozoulenko, M.; Fahlman, M.; Murphy, P. J.; Berggren, M.; Crispin, X. Semi-Metallic Polymers. *Nat. Mater.* **2014**, *13*, 190−194.

(5) Gao, C.; Chen, G. Conducting Polymer/Carbon Particle Thermoelectric Composites. *Compos. Sci. Technol.* **2016**, *124*, 52−70.

(6) Ryu, Y.; Yin, L.; Yu, C. Dramatic Electrical Conductivity Improvement of Carbon Nanotube Networks by Simultaneous De-Bundling and Hole-Doping with Chlorosulfonic Acid. *J. Mater. Chem.* **2012**, *22*, 6959−6964.

(7) Hu, X.; Chen, G.; Wang, X.; Wang, H. Tuning Thermoelectric Performance by Nanostructure Evolution of a Conducting Polymer. *J. Mater. Chem. A* **2015**, *3*, 20896−20902.

(8) McGrail, B. T.; Sehirlioglu, A.; Pentzer, E. Polymer Composites for Thermoelectric Applications. *Angew. Chem., Int. Ed.* **2015**, *54*, 1710−1723.

(9) Xu, K.; Chen, G.; Qiu, D. Convenient Construction of Poly (3, 4-ethylenedioxythiophene)−Graphene Pie-Like Structure with En-

DOI: 10.1021/acsnano.7b01279
ACS Nano 2017, 11, 5746−5752

hanced Thermoelectric Performance. *J. Mater. Chem. A* **2013**, *1*, 12395−12399.
(10) Glaudell, A. M.; Cochran, J. E.; Patel, S. N.; Chabinyc, M. L. Impact of the Doping Method on Conductivity and Thermopower in Semiconducting Polythiophenes. *Adv. Energy Mater.* **2015**, *5*, 1401072.
(11) Gao, C.; Chen, G. A New Strategy to Construct Thermoelectric Composites of SWCNTs and Poly-Schiff Bases with 1, 4-Diazabuta-1, 3-Diene Structures Acting as Bidentate-Chelating Units. *J. Mater. Chem. A* **2016**, *4*, 11299−11306.
(12) He, M.; Qiu, F.; Lin, Z. Towards High-Performance Polymer-Based Thermoelectric Materials. *Energy Environ. Sci.* **2013**, *6*, 1352−1361.
(13) Xu, K.; Chen, G.; Qiu, D. *In situ* Chemical Oxidative Polymerization Preparation of Poly (3, 4-ethylenedioxythiophene)/Graphene Nanocomposites with Enhanced Thermoelectric Performance. *Chem. - Asian J.* **2015**, *10*, 1225−1231.
(14) Liang, L.; Chen, G.; Guo, C.-Y. Enhanced Thermoelectric Performance by Self-Assembled Layered Morphology of Polypyrrole Nanowire/Single-Walled Carbon Nanotube Composites. *Compos. Sci. Technol.* **2016**, *129*, 130−136.
(15) Liang, L.; Gao, C.; Chen, G.; Guo, C.-Y. Large-Area, Stretchable, Super Flexible and Mechanically Stable Thermoelectric Films of Polymer/Carbon Nanotube Composites. *J. Mater. Chem. C* **2016**, *4*, 526−532.
(16) Zhang, Z.; Chen, G.; Wang, H.; Zhai, W. Enhanced Thermoelectric Property by the Construction of a Nanocomposite 3D Interconnected Architecture Consisting of Graphene Nanolayers Sandwiched by Polypyrrole Nanowires. *J. Mater. Chem. C* **2015**, *3*, 1649−1654.
(17) Zhang, Z.; Chen, G.; Wang, H.; Li, X. Template-Directed *in situ* Polymerization Preparation of Nanocomposites of PEDOT:PSS-Coated Multi-Walled Carbon Nanotubes with Enhanced Thermoelectric Property. *Chem. - Asian J.* **2015**, *10*, 149−153.
(18) Li, J.; Lai, C.; Xiang, X.; Wang, L. Synthesis and Characterization of Poly-Schiff Bases with a Donor-Acceptor Structure Containing Thiophene Units as Thermoelectric Materials. *J. Mater. Chem. C* **2015**, *3*, 2693−2701.
(19) Li, J.; Lai, C.; Jia, X.; Wang, L.; Xiang, X.; Ho, C.-L.; Li, H.; Wong, W.-Y. Effect of Electron Donor/Acceptor Substituents on the Seebeck Coefficient and Thermoelectric Properties of Poly(3-methylthiophene methine)s/Graphite Composites. *Composites, Part B* **2015**, *77*, 248−256.
(20) Montgomery, D. S.; Hewitt, C. A.; Barbalace, R.; Jones, T.; Carroll, D. L. Spray Doping Method to Create a Low-Profile High-Density Carbon Nanotube Thermoelectric Generator. *Carbon* **2016**, *96*, 778−781.
(21) Nonoguchi, Y.; Ohashi, K.; Kanazawa, R.; Ashiba, K.; Hata, K.; Nakagawa, T.; Adachi, C.; Tanase, T.; Kawai, T. Systematic Conversion of Single Walled Carbon Nanotubes into N-Type Thermoelectric Materials by Molecular Dopants. *Sci. Rep.* **2013**, *3*, 3344.
(22) Wu, G.; Gao, C.; Chen, G.; Wang, X. High-Performance Organic Thermoelectric Modules Based on Flexible Films of a Novel N-Type Single-Walled Carbon Nanotube. *J. Mater. Chem. A* **2016**, *4*, 14187−14193.
(23) Zhang, F.; Zang, Y.; Huang, D.; Di, C.-A.; Di, X.; Sirringhaus, H.; Zhu, D. Modulated Thermoelectric Properties of Organic Semiconductors Using Field-Effect Transistors. *Adv. Funct. Mater.* **2015**, *25*, 3004−3012.
(24) Shi, K.; Zhang, F.; Di, C.-A.; Yan, T.-W.; Zou, Y.; Zhou, X.; Zhu, D.; Wang, J.-Y.; Pei, J. Toward High Performance N-Type Thermoelectric Materials by Rational Modification of BDPPV Backbones. *J. Am. Chem. Soc.* **2015**, *137*, 6979−6982.
(25) Schlitz, R. A.; Brunetti, F. G.; Glaudell, A. M.; Miller, P. L.; Brady, M. A.; Takacs, C. J.; Hawker, C. J.; Chabinyc, M. L. Solubility-Limited Extrinsic N-Type Doping of a High Electron Mobility Polymer for Thermoelectric Applications. *Adv. Mater.* **2014**, *26*, 2825−2830.
(26) Zhang, Z.-G.; Qi, B.; Jin, Z.; Chi, D.; Qi, Z.; Li, Y.; Wang, J. Perylene Diimides: a Thickness-Insensitive Cathode Interlayer for High Performance Polymer Solar Cells. *Energy Environ. Sci.* **2014**, *7*, 1966−1973.
(27) Zhan, X.; Facchetti, A.; Barlow, S.; Marks, T. J.; Ratner, M. A.; Wasielewski, M. R.; Marder, S. R. Rylene and Related Diimides for Organic Electronics. *Adv. Mater.* **2011**, *23*, 268−284.
(28) Russ, B.; Robb, M. J.; Brunetti, F. G.; Miller, P. L.; Perry, E. E.; Patel, S. N.; Ho, V.; Chang, W. B.; Urban, J. J.; Chabinyc, M. L.; Hawker, C. J.; Segalman, R. A. Power Factor Enhancement in Solution-Processed Organic N-Type Thermoelectrics Through Molecular Design. *Adv. Mater.* **2014**, *26*, 3473−3477.
(29) Collins, P. G.; Bradley, K.; Ishigami, M.; Zettl, A. Extreme Oxygen Sensitivity of Electronic Properties of Carbon Nanotubes. *Science* **2000**, *287*, 1801−1804.
(30) Bradley, K.; Jhi, S.-H.; Collins, P. G.; Hone, J.; Cohen, M. L.; Louie, S. G.; Zettl, A. Is the Intrinsic Thermoelectric Power of Carbon Nanotubes Positive? *Phys. Rev. Lett.* **2000**, *85*, 4361−4364.
(31) Wang, C.; Zhou, G.; Liu, H.; Wu, J.; Qiu, Y.; Gu, B.-L.; Duan, W. Chemical Functionalization of Carbon Nanotubes by Carboxyl Groups on Stone-Wales Defects: a Density Functional Theory Study. *J. Phys. Chem. B* **2006**, *110*, 10266−10271.
(32) Yu, C.; Murali, A.; Choi, K.; Ryu, Y. Air-Stable Fabric Thermoelectric Modules Made of N-and P-Type Carbon Nanotubes. *Energy Environ. Sci.* **2012**, *5*, 9481−9486.
(33) Wang, H.; Hsu, J.-H.; Yi, S.-I.; Kim, S. L.; Choi, K.; Yang, G.; Yu, C. Thermally Driven Large N-Type Voltage Responses from Hybrids of Carbon Nanotubes and Poly (3, 4-ethylenedioxythiophene) with Tetrakis(dimethylamino) ethylene. *Adv. Mater.* **2015**, *27*, 6855−6861.
(34) Nonoguchi, Y.; Nakano, M.; Murayama, T.; Hagino, H.; Hama, S.; Miyazaki, K.; Matsubara, R.; Nakamura, M.; Kawai, T. Simple Salt-Coordinated N-Type Nanocarbon Materials Stable in Air. *Adv. Funct. Mater.* **2016**, *26*, 3021−3028.
(35) Piao, M. X.; Joo, M. K.; Choi, J. H.; Shin, J. M.; Moon, Y. S.; Kim, G. T.; Weglikowska, U. D. Evaluation of Power Generated by Thermoelectric Modules Comprising a P-Type and N-Type Single Walled Carbon Nanotube Composite Paper. *RSC Adv.* **2015**, *5*, 78099−78103.
(36) Hewitt, C. A.; Montgomery, D. S.; Barbalace, R. L.; Carlson, R. D.; Carrol, D. L. Improved Thermoelectric Power Output from Multilayered Polyethylenimine Doped Carbon Nanotube Based Organic Composites. *J. Appl. Phys.* **2014**, *115*, 184502.

DOI: 10.1021/acsnano.7b01279
ACS Nano 2017, 11, 5746−5752